Chinese Journal of Chemical Engineering 90 (2026) 94–105

Contents lists available at ScienceDirect

Chinese Journal of Chemical Engineering

journal homepage: www.elsevier.com/locate/CJChE

Full Length Article

Analysis of the competitive reaction rates of dibenzothiophene and naphthalene in the hydrodenitrogenation of 1,2,3,4-tetrahydroquinoline over Pt-based catalysts

Yifan Xue [1], Fei Zhao [1], Jie Feng [1, 2, 3, *], Wenying Li [1, 2, 3]

[1] State Key Laboratory of Clean and Efficient Coal Utilization, Taiyuan University of Technology, Taiyuan 030024, China
[2] Beijing Huairou Laboratory, Beijing 101499, China
[3] Shanxi Research Institute of Huairou Laboratory, Taiyuan 030032, China

ARTICLE INFO

Article history:
Received 28 May 2025
Received in revised form
28 September 2025
Accepted 28 September 2025
Available online 9 December 2025

Keywords:
Nitrogen adsorption
C–N bond cleavage
Competitive adsorption
HDS
Hydrogenation
Kinetic modeling

ABSTRACT

In hydrofining processes, the competitive interactions among sulfur-containing compounds, aromatic hydrocarbons, and nitrogen-containing intermediates fundamentally govern catalytic performance. Nevertheless, the complex kinetic relationships within hydrodenitrogenation (HDN) systems have remained unclear and insufficiently investigated. This research comprehensively and systematically examined the competitive reaction kinetics of naphthalene (an aromatic model) and dibenzothiophene (a sulfur-based model) during the HDN of 1,2,3,4 - tetrahydroquinoline over Pt-based catalysts. Through systematic analysis of conversion rates and product distributions across various reaction conditions, it demonstrated that both dibenzothiophene and naphthalene exert distinct inhibitory effects on HDN through mechanistically differentiated pathways. Quantitative evaluation revealed a pronounced temperature dependence in mitigating these inhibitory effects, whereas pressure variations exhibited negligible influence. These findings collectively demonstrate that surface adsorption competition, rather than hydrogen availability, dictates the reaction kinetics. Rigorous kinetic calculations and rate constant fittings identified the hydrogenation of 1,2,3,4-tetrahydroquinoline to decahydroquinoline as the rate-limiting step susceptible to competitive inhibition. This phenomenon predominantly arises from the tripartite competitive adsorption among naphthalene, dibenzothiophene, and 1,2,3,4-tetrahydroquinoline at catalytic active sites, as corroborated by theoretical adsorption energy calculations. Notably, the two inhibitors manifest divergent interaction mechanisms: H^+ ions generated during H_2S formation in dibenzothiophene desulfurization facilitate C–N bond cleavage, whereas naphthalene directly suppresses this critical step. Furthermore, atomic-layer-deposited TiO_2 on Pt/Al_2O_3 engineered the catalyst surface through three synergistic effects: enhanced nitrogen adsorption capacity, optimized hydrogen spillover, and generation of additional C–N bond cleavage sites. This multi-effect strategy effectively reduces the negative impacts of competitive adsorption, emphasizing the crucial role of competitive reaction kinetics in designing sulfur/aromatic-resistant HDN catalysts.

1. Introduction

The primary liquid products resulting from direct coal conversion technology are coal-based liquids, including coal tar and direct coal liquefaction oil. These liquids have great potential for applications [1], which can be employed in the preparation of high-energy-density fuels through the application of hydrofining, hydrogenation and hydro-isomerization reactions. Sulfur-containing molecules, nitrogen-containing compounds, and unsaturated aromatic hydrocarbons frequently coexist during the hydrofining process of crude oil. As a result, the hydrodesulfurization (HDS), hydrodenitrogenation (HDN), and hydrogenation reactions occur simultaneously in the same section, and there is a certain level of interaction between these reactions [2–4]. Such interactions often lead to competitive adsorption on catalyst surfaces, reducing the simultaneous removal efficiency. This inefficiency not only increases energy consumption but also

* Corresponding author.
E-mail address: fengjie@tyut.edu.cn (J. Feng).

https://doi.org/10.1016/j.cjche.2025.09.037

necessitates additional purification steps, thus contradicting the principles of green chemistry that prioritize atom economy and waste minimization. An understanding of these interactions can inform the design of more efficient catalytic processes, where competition between different reactions can be avoided and overall catalytic activity is enhanced.

Because of their potent adsorption on active sites [5], nitrogen compounds are well-known HDS inhibitors over sulfide catalysts; however, their function in HDN systems under sulfur/aromatic co-feeding circumstances is still unclear [6,7]. Most experts in this field have conducted in - depth and meticulous studies on the impact of nitrogen - containing substances on the HDS reaction. The findings indicate that nitrogen heterocycles exhibit a stronger binding affinity to the catalytic site compared to aromatics and organosulfur compounds, thereby exerting an inhibitory effect on HDS. The initial observation of this phenomenon was made in 1975 by researchers [8], who discovered that pyridine exerted an inhibitory effect on the HDS reaction of thiophene, irrespective of the type of sulfide catalyst employed. The monocyclic molecule pyridine, in its gaseous form, along with NH_3 molecules [9], exocyclic nitrogen-containing molecules such as aniline and polycyclic nitrogen-containing compounds quinoline (Q), all function as inhibitors of the HDS reaction of thiophene. The strength of inhibition follows the order Q > pyridine > aniline > NH_3 [10], with a positive correlation trend with the basicity of the nitrogen-containing molecules. Numerous investigations have shown that the basicity of the nitrogen-containing substances directly correlates with the degree of inhibition of the HDS process [11–13]. Additionally, research on non-basic nitrogen-containing substances has shown that they simultaneously impede the HDS process [14]. Nevertheless, kinetic studies have demonstrated that the inhibition is independent of proton affinity [15]. Moreover, research has shown a linear relationship between nitrogen-containing heterocycles' adsorption equilibrium constants and their proton affinity over MoS_2 catalysts [16]. In the dibenzothiophene (DBT) HDS process, two distinct inhibition pathways have been identified: a hydrogenation path and a direct desulfurization path. Compounds containing nitrogen have a stronger inhibitory effect on the hydrogenation active site, whereas the active site of direct bond-breaking is less affected. The active site of bond-breaking is inhibited to a lesser extent, and therefore sulfur-containing compounds that rely on the desulfurization of the direct bond-breaking are less affected. In contrast, the inhibition effect of sulfur-containing compounds with a substituent group, which mainly rely on the hydrogenation pathway for desulfurization, is strongly inhibited [12,17].

Paradoxically, certain nitrogen species and aromatics have been reported to enhance HDS activity [7]. According to the study, under some circumstances, nitrogen-containing substances like as acridine, Q molecules, and 2-methylpyridine or 2-methylpiperidine can aid in the HDS of DBT [18]. It was demonstrated that both alkaline and non-alkaline nitrogen-containing compounds could facilitate the HDS on Ni-MoS_2/Al_2O_3. The pathway through which this promotion occurred was predominantly the direct desulfurization pathway [7]. The apparent rate constant of the HDS hydrogenation pathway (HYD) increased in the presence of naphthalene (NP). However, this chemical pathway was inhibited when nitrogen-containing substances were present [19,20]. Lower reaction temperatures facilitate the promotion of DBT desulfurization by non-basic nitrogenous compounds and unsaturated aromatic hydrocarbons. In contrast, the effect of temperature on DBT desulfurization in the presence of basic nitrogenous compounds is not unidirectional, but rather exhibits a volcano-shaped curve [7]. The preceding studies have demonstrated a multifaceted kinetic relationship between the hydrogenation, desulfurization and denitrogenation pathways. This kinetic ambiguity has been shown to impede the development of hydrorefining. Consequently, it is imperative to address this lacuna to facilitate the advancement of the clean and efficient utilization of coal-based liquids.

Platinum-based catalysts have significant potential in HDN and HDS reactions during hydrogenation processes. The situation with noble metal catalysts differs from that with sulfide catalysts. Infantes-Molina *et al.* [21] studied HDN and HDS activity on RuS_2 and found that the presence of Q molecules had little impact on the HDS reactivity. However, when DBT was present, HDN reactivity increased. The findings showed that the HDS and HDN reactions occurred at distinct active sites and the reaction pathways were markedly disparate. Different concentrations of DBT were introduced at different stages of the HDN reaction of Q, which was conducted over a Pt/Al_2O_3 catalyst [22]. In the Pt-based catalysts, the selectivities for o-propylaniline (OPA) and PB are both found to be low, indicating that 1,2,3,4-tetrahydroquinoline (14THQ) undergoes hydrogenation to form decahydroquinoline (DHQ), followed by hydrogenolysis ring-opening for denitrogenation. In the Pt-based catalysts, the selectivity for the hydrogenated saturated product, DHQ, exhibits a marked enhancement in comparison to that observed in sulfide catalysts. As the temperature rises, the bond-breaking process is enhanced, and the selectivity for DHQ gradually decreases. It was established that the HDN reactivity diminished with the incorporation of DBT. Subsequent analysis of the intermediate products indicated that the presence of DBT predominantly impeded the subsequent hydrogenation of tetrahydroquinoline, thereby preventing the formation of DHQ. The investigation revealed that both species exhibited comparable adsorption energies, indicating a competitive adsorption effect. Consequently, it was hypothesized that the decrease in activity of the HDN reaction upon the addition of DBT could be attributed not to catalyst deactivation but to the surface active sites' competing adsorption impact [23]. This underscores the necessity for an examination of the reaction kinetics mechanism.

In the present study, DBT (a sulfur-containing compound) and NP (an unsaturated aromatic hydrocarbon) were introduced as model compounds into the reaction system. This work sought to determine the competitive kinetics of the HDN reaction of 14THQ over Pt-based catalysts. Through the analysis of conversion and product yields under varied conditions, it was demonstrated that both DBT and NP inhibit the HDN reaction through distinct mechanisms. Through the analysis of reaction parameters (temperature/pressure) and their correlation with inhibition, it was determined that inhibition decreases with increasing temperature, while the effect of pressure variation is negligible. This suggests that surface adsorption competition, rather than hydrogen supply, is the primary factor influencing the reaction. Kinetic calculations and density functional theory (DFT) simulations identified the primary step in the occurrence of inhibition was determined to be the hydrogenation of 14THQ to DHQ. The fundamental mechanism for the inhibition was found to be the competing adsorption of NP, DBT, and 14THQ on the catalyst surface. This conclusion was further substantiated by theoretical calculation of adsorption energies. The calculated rate constants further elucidated that the addition of naphthalene inhibited breaking of the C–N bond, whereas the primordial step of C–N bond breaking was made easier by the addition of DBT. This was ascribed to the H^+ introduced by the desulfurization products, which favored C–N bond breaking.

2. Experimental

2.1. Materials

Al_2O_3, 1,2,3,4-tetrahydroquinoline (97%), decane (>99%, GC), PtN_2O_6 were purchased from Aladdin (Shanghai, China).

Decane was used as the solvent to create a reactant solution with 500 mg·L^{-1} of nitrogen. S concentrations in the reaction were 200 mg·L^{-1} and 1000 mg·L^{-1}. Concentration of NP in the reactants is 1% mass fraction.

2.2. Catalyst preparation

The purchased γ-Al_2O_3 carrier was roasted for 4 h at 500 °C in a muffle furnace. An appropriate amount of precursor platinum nitrate solution was added into a beaker with 1 g of γ-Al_2O_3 carrier to ensure 1% loading of metal Pt. The solvent was evaporated and dried for 12 h at 60 °C after 1.8 g of ultrapure water was added for stirring. To create the dry catalysts, the catalysts were reduced for an hour at 500 °C in a tube furnace. The loaded Pt/Al_2O_3 catalyst was obtained. A lab FH-2 atomic layer deposition equipment was used to do ALD deposition of TiO_2 on the reduced catalyst. The deposition procedure was as follows: the titanium isopropoxide precursor was maintained at 40 °C in the precursor tank, which was supplied with high-purity nitrogen. The ultrapure water precursor was maintained at room temperature and normal pressure, with some extraction of water vapor when the vacuum was maintained through the reactor. The reactor chamber was first kept at 150 °C, the tank containing the titanium precursor was kept at 40 °C, and the water precursor tank was maintained at ambient temperature. The deposition was carried out in one single run. The deposition reaction was carried out, and the single deposition cycle consisted of four steps: (i) precursor A entered the reaction chamber, (ii) nitrogen was purged, (iii) precursor B entered the reaction chamber, and (iv) nitrogen was purged. The time of the four steps was 30-40-30-40 s [24–26]. The above steps were repeated after the end of the single deposition, and TiO_2 was deposited on the substrate for 10 cycles to obtain the catalysts named 10cTi-PtAl, respectively after the deposition.

2.3. Evaluation of the hydrodenitrogenation activity

To perform the 14THQ HDN reactions, a 300 ml tank reactor with a stirrer and a separate feedstock tank was utilized. The feedstock was provided at a reaction temperature, and samples were taken at predefined reaction durations. In the experiment, the reactor was filled with the liner that contained the catalyst and solvent, and the feed tank was filled following the solvent dissolution of the reactant. The findings of the computations in the earlier study [27] demonstrate that diffusion does not limit the reaction. After that, H_2 raised the pressure to 3 MPa. When the temperature reached 320 °C, the ball valve was opened to allow the reactant to enter the reactor. Samples were taken every 10 min during the initial 1-h reaction and every hour thereafter until the reaction stopped after 4 h [26]. The reactants NP and 14THQ solution were introduced into the feed tank in conjunction with 20 ml of decane solvent. The remaining 80 ml of solvent and catalyst were subsequently transferred to the reactor body and charged, after which the reactor was warmed up. The remainder of the procedure was identical to that employed in the HDN reaction alone. The sulfur-containing compound DBT was added in a manner analogous to that employed for NP.

The reaction products are collected as liquid products from the reactor using a real-time sampling device at a specific reaction time. The obtained liquid products are then analyzed for qualitative and quantitative determination using an Agilent 8890-5977A gas chromatography-mass spectrometry (GC-MS) system. The Agilent GC-MS system utilizes an HP-5 column (30 m × 0.25 mm × 0.25 μm) and a flame ionization detector (FID). The primary measurement parameters are as follows: injection port temperature of 280 °C, FID detector temperature of 300 °C, carrier gas N_2 flow rate of 30 ml·min^{-1}, split ratio of 30:1, and injection volume of 0.5 μl. In order to ensure optimal separation of the products, a programmed temperature gradient method is employed. The initial temperature of the column oven is set at 60 °C for a duration of 1 min. Thereafter, the temperature is elevated at a rate of 3 °C·min^{-1} to a final temperature of 120 °C, where it is maintained for a period of 10 min. This is followed by a subsequent increase at a rate of 10 °C·min^{-1} to a maximum temperature of 200 °C, which is also held for a duration of 1 min.

A qualitative and quantitative analysis of reaction products was performed using the internal standard method. This method has been shown to provide more accurate measurement results and can eliminate errors caused by changes in operating conditions to a certain extent. In this study, tetradecane was utilized as the internal standard substance for all reactions. The internal standard calibration curve for the substances involved in the HDN HDS and hydrogenated reaction is shown in Fig. S1. This was done to enable quantitative analysis of the products. The reactants and products involved in the HDN reaction include Q, 14THQ, 5,6,7,8-tetrahydroquinoline (58THQ), DHQ, OPA, phenylbenzene (PB), and propylcyclohexane (PCH). These substances were prepared as standard solutions at concentrations of 0.2, 0.4, 0.6, 0.8, and 1.0 mg·ml^{-1}. The preparation of internal standard calibration curves for the substances involved in the HDS reaction of DBT and the hydrogenation of naphthalene is essential for enabling quantitative analysis of the products. The substances primarily involved in the HDS reaction of DBT include DBT, biphenyl (BP), cyclohexylbenzene (CHB), and bicyclohexane (BCH), while the substances primarily involved in the hydrogenation and saturation of NP include NP, tetralin, and decalin. Standard solutions of the aforementioned substances should be prepared at concentrations of 0.2, 0.4, 0.6, 0.8, and 1.0 mg·ml^{-1}, and a solution of tetradecane at a concentration of 0.5 mg·ml^{-1} should be prepared. The correction factor is to be calculated on the basis of the concentrations of the standard samples and internal standards, as well as their peak areas.

2.4. DFT calculations

The adsorption energy barriers and bond dissociation energies of 14THQ and DHQ molecules on TiO_2-modified Pt(2 1 1) surfaces were computationally investigated through density functional theory (DFT) simulations implemented in Materials Studio's Dmol^3 module. In the previous study, it was found that surfaces with step sites have a higher ability to activate C–N bonds, so Pt(2 1 1) surfaces were used to simulate the adsorption activation process. The electronic exchange-correlation interactions were modeled using the Perdew-Burke-Ernzerhof (PBE) parameterization within the generalized gradient approximation (GGA) framework. Core electrons of metallic components were represented through DFT semi-core pseudopotentials (DSPP), while full-electron basis sets were applied to light elements (C, H, N, S). Valence electron orbitals were expanded using Double Numerical basis sets incorporating polarization functions (DNP). The Monkhorst-Pack mesh of k points for each model was (3 × 3 × 1). Structural optimization convergence criteria were set at energy variations below 1 × 10^{-5} Ha (1 Ha = 10^4 m^2), atomic displacement thresholds under 0.005 Å (1 Å = 0.1 nm), and force tolerances less than 0.002 Ha·Å^{-1}. The self-consistent field (SCF) calculation

precision reached 1×10^{-5} Ha [28]. The surface model was constructed by cleaving bulk platinum along the [2 1 1] crystallographic orientation, generating a six-layer slab configuration. To simulate realistic surface dynamics, the upper three atomic layers were permitted full relaxation while immobilizing the lower three layers. A vertical vacuum spacing of 14 Å along the *Z*-axis effectively eliminated inter-slab interactions. The test results for different vacuum thicknesses are shown in Table S1. A p(2 × 4) supercell architecture was implemented to model the extended Pt(2 1 1) surface environment. Three distinct adsorption geometries were systematically examined: bridge coordination sites, face-centered cubic (fcc) tri-coordination positions, and hexagonal close-packed (hcp) binding configurations.

3. Results and Discussion

3.1. Competitive effects of naphthalene on HDN under different reaction conditions

3.1.1. Effect of reaction temperature

The investigation focused on the impact of reaction temperature on reactivity, and the role of aromatics on the HDN reaction at varying temperatures. To this end, the temperature was varied from 300 to 340 °C at 20 °C intervals. Fig. 1(a) presents the results of the conversion of 14THQ HDN and the addition of aromatics after 60 min at different temperatures. The time-dependent 14THQ conversion rate is shown in Fig. S2. It is clear that an initial increase in temperature resulted in a higher conversion rate, followed by a subsequent decline. The highest conversion was recorded at 320 °C, however the reaction conversion was decreased when NP was added, suggesting that NP impedes the HDN reaction. The conversion decreased by 43.41% and 45.89% at 300°C and 320 °C, respectively, while it decreased by only 4.82% when the temperature rose to 340 °C. According to the findings, the HDN reaction benefited from the addition of NP. Based to the research results, raising the temperature might be a good way to lessen the HDN-inhibiting effects of aromatic compounds.

Regarding the reaction pathways of 14THQ HDN, three pathways are preferentially favored, as illustrated in Fig. 2. The initial pathway entails direct bond breaking, yielding OPA and PB as the predominant reaction products. The second pathway is hydrogenation bond breaking, and the main reaction products are DHQ with PCH. The third pathway is the hydrogenation reaction, and the main products are Q and 58THQ.

The yield data of the HDN reaction after 60 min for different products, as shown in Fig. 3, shows that the reactants only underwent hydrogenation to the saturated product stage at a reaction temperature of 300 °C. The time-dependent product yields are shown in Fig. S3, S4 and S5. The product was predominantly DHQ, and no denitrogenation was conducted during this period. Conversely, at a reaction temperature of 320 °C, the DHQ yield decreased and the PCH yield increased, indicative of a greater number of C—N bonds being broken at this higher temperature. At an elevated temperature of 340 °C, the yields of the direct bond-breaking compounds OPA and PB increased, and the hydrogenation reaction accounted for a significantly higher percentage, resulting in higher Q yields. Concurrently, 58THQ was generated by hydrogenating the benzene ring in Q. As the bond-breaking reaction absorbs heat, the yields of the denitrogenation products PB and PCH progressively increased as the temperature rose.

Upon the addition of the reactant NP, the overall observed trend was analogous to that of the 14THQ HDN reaction alone. The hydrogenation product DHQ predominated at reaction temperatures of 300°C and 320 °C, while the yields of the bond-breaking product PCH and the dehydrogenation products Q and 58THQ were significantly higher at 340 °C. Furthermore, it was observed that at the reaction temperature of 340 °C, the yields of DHQ and PCH decreased to a lesser extent, but the yield of Q increased and the yield of 58THQ decreased. These yield data suggest that an increase in temperature is beneficial in alleviating the inhibition of the HDN reaction by aromatic addition. In the context of the direct bond-breaking pathway, the overall yields of the products OPA and PB were found to be minimal at 300°C and 320 °C, respectively. The addition of NP led to a decline in yield at 340 °C, thereby further substantiating the hypothesis that the NP addition inhibits the C—N bond breaking process.

3.1.2. Effect of reaction pressure

The present study investigates the impact of reaction pressure on reaction activity and the effect of aromatics on the HDN reaction at varying pressures. The experiment was conducted by systematically varying the pressure from 3 to 6 MPa. As illustrated in Fig. 3, the yield of 14THQ HDN reaction after 60 min products at varying pressures was examined. It was shown that the hydrogenation bond breaking route predominated in the HDN reaction as

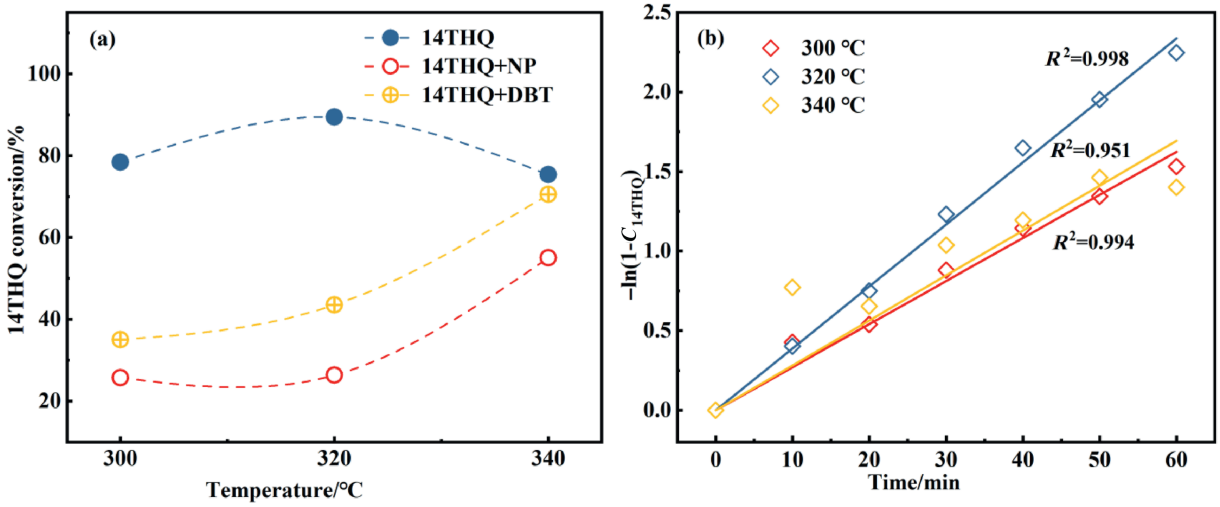

Fig. 1. (a) The 14THQ HDN conversion. (b) 14THQ disappearance first-order plot during HDN of 14THQ over Pt/Al_2O_3.

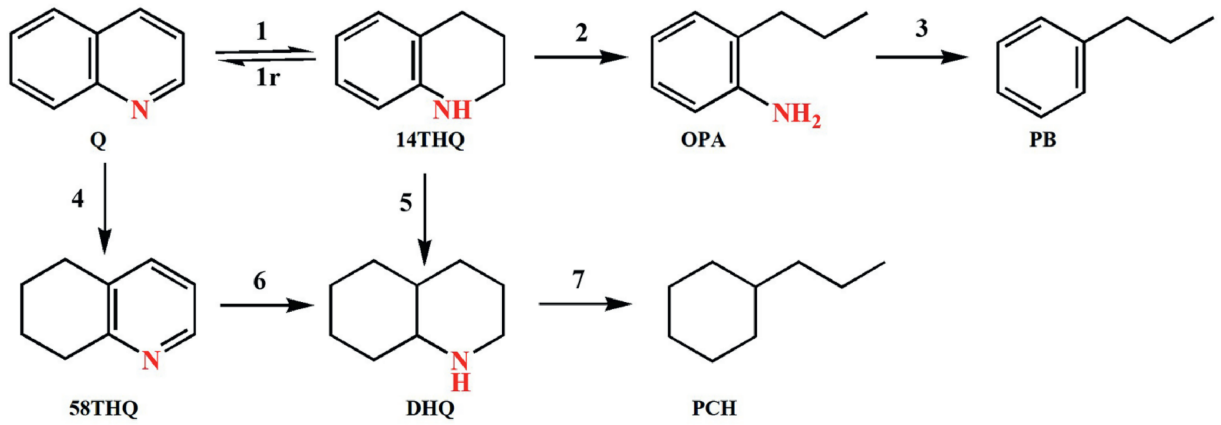

Fig. 2. 14THQ HDN reaction network.

pressure increased, leading to an elevated yield of PCH. Following the addition of NP, the reaction path remained largely unchanged, with a decrease in the DHQ yield of 30.44% and 32.62% at 3 MPa and 6 MPa, respectively, while the PCH yield decreased by 2.28% and 1.36%, respectively. In the direct bond breaking and hydrogenation reaction pathway, the yields of certain products remained largely unchanged, with only the 58THQ yield increasing by 2.72% and 1.91%, respectively. These findings suggest that the inhibition of NP on the HDN reaction was not significantly alleviated by elevated pressure.

3.1.3. Hydrogenation of naphthalene

The hydrogenation reaction path of NP is illustrated in Fig. 4, yielding two primary products, tetralin and decalin. A detailed analysis of the hydrogenation process and products of the added reactants naphthalene was conducted, and it was ascertained that the majority of naphthalene was hydrogenated to create incompletely saturated tetralin in the presence of nitrogen-containing compounds. The tetralin yields of the products at varying temperatures and pressures after 60 min are presented in Table 1, which demonstrates that yields increase and subsequently decrease with rising temperature, with the maximum yield at 320 °C, and a substantial increase with increasing pressure.

The analysis of NP hydrogenation products through the aforementioned process revealed that the yield of tetralin was low at 340 °C, indicating that the hydrogenation reaction was unfavorable at this temperature. Concurrently, the competitive effect of the hydrogenation saturation reaction on the HDN reaction was reduced. However, an increase in reaction pressure led to an enhancement in the yield of NP hydrogenation products. This observation indicates that the inhibition of NP on the HDN reaction is not mitigated by altering the reaction pressure. This finding suggests that the reaction pressure intervals that are conducive to the HDN and hydrogenation reactions have a congruent nature, thereby implying that modifying the pressure does not serve as an effective strategy for alleviating the inhibition. Consequently, the process conditions can be modified by selecting temperature intervals for both reactions to achieve higher yields of hydrogenation or denitrogenation products.

3.2. Mechanism of naphthalene inhibition on hydrodenitrogenation reaction

3.2.1. Model development

Fig. 1(b) shows a distinct linear connection between $-\ln(1-C_{14THQ})$ and reaction time at three distinct temperatures. In this case, the conversion of 14THQ is shown as C_{14THQ}. The majority of experimental data points may be precisely aligned along a corresponding straight line within the given error range, suggesting that the 14THQ HDN conversion satisfies the requirements for a first-order reaction. The rate constant was found to be the line gradient. As a result, the rate constants for the conversion of 14THQ at 300, 320, and 340 °C were found to be 0.0271, 0.0389, and 0.0282 min^{-1}, respectively. The results showed that the R^2 values were, correspondingly, 0.994, 0.998, and 0.951.

As demonstrated in the preceding sections, experimental data has been analyzed in order to determine the three primary pathways for the 14THQ HDN reaction. The reaction network displayed in Fig. 2 serves as the basis for the development of the kinetics model for HDN of 14THQ over Pt/Al_2O_3 catalyst. The reaction pathways are described in detail by the chemical equations below:

$$C_9H_7N(Q) + 2H_2 \xrightarrow{k_1} C_9H_{11}N(14THQ)$$

$$C_9H_{11}N(14THQ) \xrightarrow{k_{1r}} C_9H_7N(Q) + 2H_2$$

$$C_9H_{11}N(14THQ) + H_2 \xrightarrow{k_2} C_9H_{13}N(OPA)$$

$$C_9H_{13}N(OPA) + H_2 \xrightarrow{k_3} C_9H_{12}(PB) + NH_3$$

$$C_9H_7N(Q) + 2H_2 \xrightarrow{k_4} C_9H_{11}N(58THQ)$$

$$C_9H_{11}N(14THQ) + 3H_2 \xrightarrow{k_5} C_9H_{17}N(DHQ)$$

$$C_9H_{11}N(58THQ) + 3H_2 \xrightarrow{k_6} C_9H_{17}N(DHQ)$$

$$C_9H_{17}N(DHQ) + 2H_2 \xrightarrow{k_7} C_9H_{18}(PCH) + NH_3$$

The example below displays a reaction rate equation for the designated route in its generic form [29,30]:

$$r = -\frac{dn_A}{\xi m_{cat} dt} = kC_A^a C_B^b$$

The symbols r, n_A, and ξ stand for the reaction rate, moles of reactant A, and reaction progress that rely on A, respectively. Reactant A and B concentrations are denoted by C_A and C_B, corresponding reaction orders by a and b, catalyst loading by m_{cat}, and

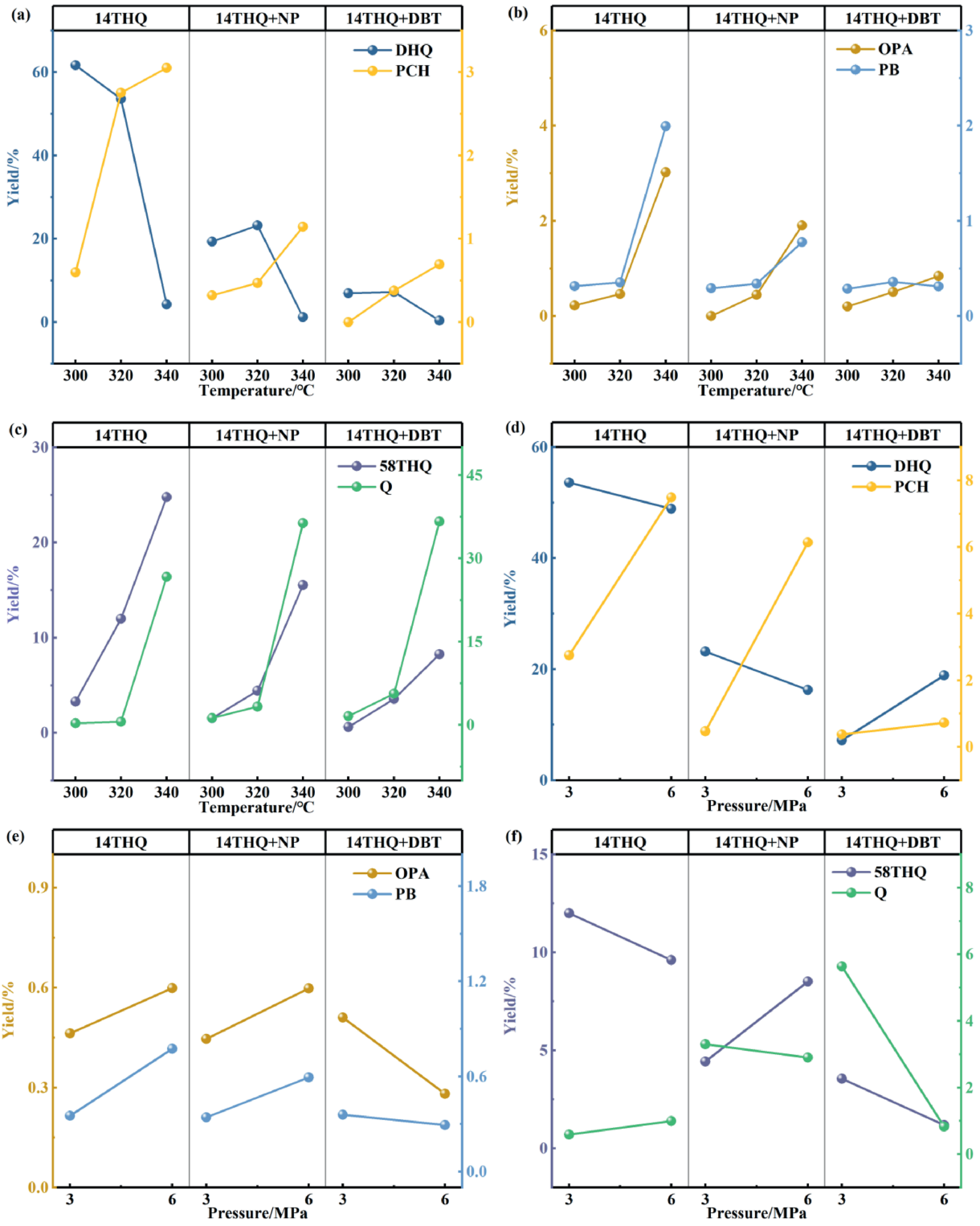

Fig. 3. HDN reaction product yields at different temperatures and pressures. (a), (d) Yields of the hydrogenation bond-breaking pathway products DHQ and PCH. (b), (e) Yields of the direct bond-breaking pathway products OPA and PB. (c), (f) Yield of the hydrogenation and dehydrogenation pathway products 58THQ and Q.

rate constant by *k*. This type of rate expression is seen in published research elsewhere [31] and is based on the assumption that a and b equal 1. The following are the differential equations that were derived. Fitting the experimental data to the differential equations produced the differential equations for each of the species that were part of this model.

$$\frac{dn_Q}{m_{cat}dt} = -k_1C_Q + k_{1r}C_{14THQ} - k_4C_Q$$

$$\frac{dn_{14THQ}}{m_{cat}dt} = -k_{1r}C_{14THQ} - k_2C_{14THQ} - k_5C_{14THQ} + k_1C_Q$$

Fig. 4. Naphthalene hydrogenation reaction pathway.

Table 1
The tetralin yields of the products at varying temperatures and pressures.

Pressure/MPa	Temperature/°C	Tetralin yield/%
3	300	12.54
	320	17.01
	340	12.33
6	320	25.28

$$\frac{dn_{58THQ}}{m_{cat}dt} = -k_6 C_{58THQ} + k_4 C_Q$$

$$\frac{dn_{DHQ}}{m_{cat}dt} = -k_7 C_{DHQ} + k_6 C_{58THQ} + k_5 C_{14THQ}$$

$$\frac{dn_{OPA}}{m_{cat}dt} = -k_3 C_{OPA} + k_2 C_{14THQ}$$

$$\frac{dn_{PB}}{m_{cat}dt} = k_3 C_{OPA}$$

$$\frac{dn_{PCH}}{m_{cat}dt} = k_7 C_{DHQ}$$

The differential equations were numerically solved using the MATLAB program, and the parameter values were estimated at the same time. The best fitting value for each path was found by minimizing the square sum error between the experimental data and the model computation. The reaction rate constant (k_1 to k_7) was defined as a parameter. Table 2 contains the estimated rate constants. In Fig. S6 of supplementary data, the fitted curves are displayed.

3.2.2. Reaction rate analysis

As demonstrated in Table 2, Path 1 exhibits the highest rate constant, signifying that Q is remarkably susceptible to conversion to 14THQ. In contrast, the rate of 14THQ hydrogenation saturation is significantly higher than the rate of Q hydrogenation to 58THQ and subsequent hydrogenation to DHQ. The comparison of the hydrogenation bond breaking and direct bond breaking pathways reveals that the reaction of 14THQ hydrogenation to DHQ is faster, suggesting that the hydrogenation and C–N cleavage pathway is more likely to be carried out under these reaction conditions. The fact that the reaction rate constants k_7 for the broken C–N bond and k_2 and k_3 in the direct bond-breaking route were both an order of magnitude lower than the hydrogenation reaction k_5 indicates that the C–N bond-breaking reaction is the step that determines the HDN reaction rate. This result is in line with earlier studies' findings that the bond-breaking reaction of heterocyclic compounds containing nitrogen is the most challenging to perform [32,33].

A detailed analysis of the reaction rate constants following the addition of NP indicates that the rate constants k_2 and k_5, which govern the initial steps of 14THQ hydrogenation bond breaking and direct bond breaking, respectively, exhibit a substantial decrease. In contrast, the initial step k_7 for breaking the C–N bond demonstrates only a minor decrease. This observation indicates that the activation of 14THQ is significantly influenced by the addition of the reactant NP, which is likely attributable to the impact of 14THQ adsorption. The analysis indicates the presence of a benzene ring in both the 14THQ molecule and NP, suggesting a competition on the surface for adsorption. The nitrogen-containing compound reaction adsorption activation site is seen to be occupied by the addition of NP. It has been demonstrated that adding nitrogen-containing compounds to the hydrogenation reaction significantly reduces the catalyst capacity to hydrogenate when N-compounds are present [34]. The weak inhibition of the C–N bond breaking process may be attributed to the fact that the 14THQ hydrogenation saturated product, DHQ, is an all-hydrogen molecule with a high steric hindrance on the surface. Following the hydrogenation of naphthalene molecules, the reaction rate is decreased because tetralin maintains its unsaturated structure and interacts strongly with the surface, occupying the DHQ molecules adsorption sites.

As shown in Fig. 5, theoretical estimates of the adsorption configurations and adsorption energies of naphthalene and tetralin were performed and compared with those of 14THQ and DHQ. The adsorption energies of 14THQ and DHQ have been calculated in the previous work. The findings indicate that naphthalene exhibits optimal stability when adsorbed on the surface in the hcp configuration, with an adsorption energy of −2.22 eV. Conversely, for tetralin, the most stable configuration is identified as bridge, corresponding to an adsorption energy of −1.70 eV. In our earlier investigation, we computed the adsorption configurations and adsorption energies of 14THQ and DHQ, and the most stable configurations are hcp and bridge, with adsorption energies of −2.24 eV, respectively, for the adsorption of tetralin on Pt(2 1 1). The most stable configurations were hcp and bridge, with adsorption energies of −2.24 and −1.60 eV on Pt(2 1 1), respectively. The higher adsorption energy of tetralin in comparison to that of DHQ suggests that, of the two intermediates, tetralin will be more readily adsorbed on the catalyst surface. As a result, DHQ adsorption will be inhibited, which will lower its reaction rate while breaking the C–N bond.

3.3. Competitive effects of dibenzothiophene on HDN under different reaction conditions

3.3.1. Effect of reaction temperature

The impact of DBT, a compound containing sulfur, on the HDN reaction at varying temperatures was examined by systematically altering the temperature. Results of the conversion of 14THQ HDN alone and the addition of DBT at various temperatures are shown in Fig. 1(a). The time-dependent 14THQ conversion rate is shown in Fig. S2. The data clearly show that adding DBT lowers the

Table 2
Optimized values of the rate constants.

Sample	Rate constant							
	k_1	k_{1r}	k_2	k_3	k_4	k_5	k_6	k_7
14THQ	2.60×10^{1}	1.99	2.77×10^{-3}	6.19×10^{-3}	7.73×10^{-2}	2.56×10^{-2}	1.00×10^{-6}	2.02×10^{-3}
14THQ + NP	5.53×10^{1}	5.62	6.49×10^{-4}	6.63×10^{-3}	1.25×10^{-2}	4.91×10^{-3}	2.87×10^{-4}	1.08×10^{-3}
14THQ + DBT	1.86×10^{1}	2.13	3.26×10^{-4}	5.93×10^{-3}	5.52×10^{-3}	1.20×10^{-3}	3.11×10^{-5}	2.30×10^{-3}

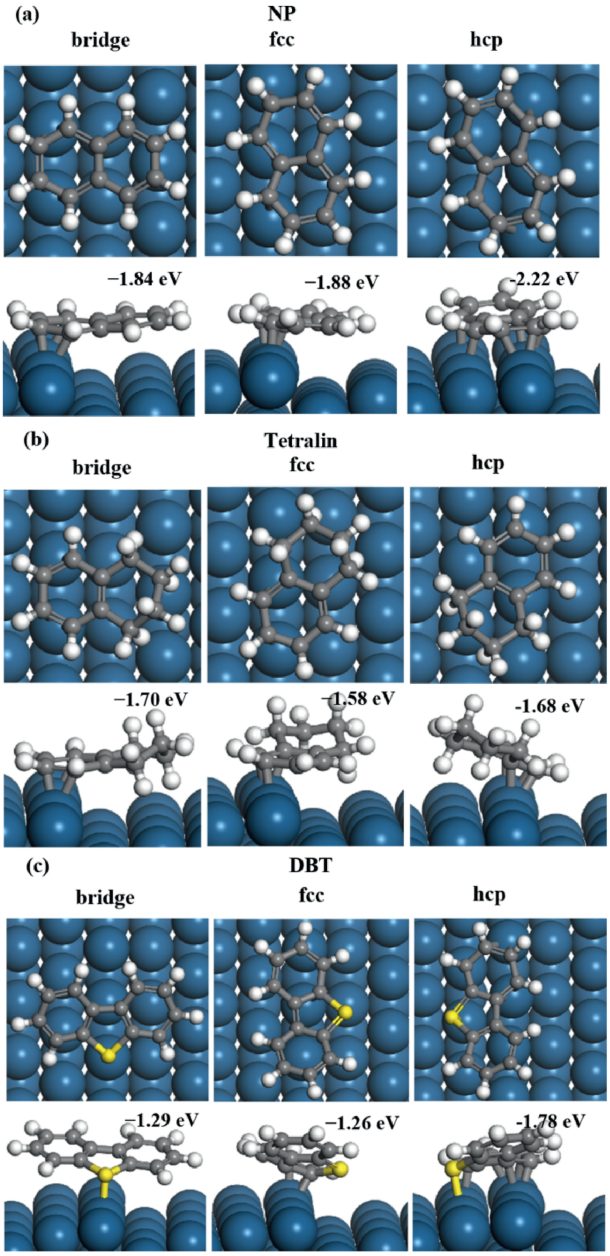

Fig. 5. Adsorption configuration of (a) NP, (b) tetralin and (c) DBT on hollow (hcp or fcc), and bridge sites of Pt (2 1 1) surfaces.

conversion of 14THQ, indicating that DBT inhibits the HDN reaction on some level. Specifically, the conversion decreased by 52.69% and 63.02% at 300 °C and 320 °C, respectively, while at 340 °C, the conversion decreased by only 20.35%. These findings suggest that an increase in temperature could alleviate the inhibitory effect of aromatics addition on the HDN.

The 14THQ HDN reaction pathway and product distribution have been analyzed in the Section 3.1.1. Following the addition of DBT, the HDN reaction products were further examined; the outcomes are shown in Fig. 3. The time-dependent product yields are shown in Fig. S3, S4 and S5. The data clearly shows that the trend of the product DHQ yield in the hydrogenation route changes as the temperature rises, first showing an increase and then a drop in yield. At 300 °C and 320 °C, the yield significantly decreases, however at 340 °C, the yield decreases less sharply. The PCH yield exhibited an overall increasing trend, with a decrease of 2.28% at 320 °C and 1.90% at 340 °C after the temperature increase. These yield data suggest that an increase in temperature is beneficial in alleviating the inhibitory effect of DBT incorporation on the HDN reaction. In the direct bond breaking pathway, the products OPA and PB demonstrated a decline in yield upon the incorporation of DBT, further substantiating the inhibitory effect of DBT on this process, as the temperature increased to 340 °C. It was found that at 340 °C, the reaction as a whole prefers to move down the bond-breaking after hydrogenation pathway. The yield of the HDN product Q remains relatively unaffected, while the yield of the Q hydrogenation product 58THQ decreases, suggesting that the addition of DBT inhibits the hydrogenation reaction but does not have an effect on the bond-breaking after hydrogenation pathway.

3.3.2. *Effect of reaction pressure*

The reaction pressure was varied in order to ascertain whether a change in pressure interval would improve the inhibition. The yield of the bond-breaking product PCH does not significantly increase with increasing pressure, according to the product yields displayed in Fig. 3, the yield of DHQ in the HDN pathway does. This finding suggests that the increase in pressure did not alleviate the inhibition of the bond-breaking process by DBT, and that the increase in DHQ yield was due to the promotion of the hydrogenation reaction by the increased pressure. Conversely, the pressure increase dramatically reduced the yield of Q for the dehydrogenation pathway to the level observed in the absence of DBT, which in turn reduced the yield of 58THQ. In contrast to the effect of aromatic NP, the yield of the hydrogenation reaction was not drastically reduced by an increase in pressure, although a reduction was still possible.

3.3.3. *Effect of sulfur content*

Coal-based liquids have been found to include both sulfur- and nitrogen-containing molecules, albeit the makeup of these chemicals varies throughout oils. In the HDN reaction of 14THQ, the concentration of N was controlled to be 500 $mg \cdot L^{-1}$. Therefore, the effect of different S contents on the HDN reaction was explored by varying the concentration of S in the addition of DBT. The product yield of concentrations of sulfur varied between 200 and 1000 $mg \cdot L^{-1}$, presented in Fig. S7, demonstrate that the change in sulfur content does not affect the reaction pathway in a general way. The hydrogenation bond-breaking pathway remains the dominant reaction, however, an increase in sulfur content results in an enhancement of the yield of denitrogenation product PB in the direct bond-breaking pathway. Concurrently, an increase in sulfur concentration was observed to result in a decline in product yields for both DHQ and PCH, thereby indicating that the presence of DBT exerts a first-order inhibition on the hydrogenation step of 14THQ to DHQ.

3.3.4. *DBT hydrodesulfurization reaction*

As demonstrated in Fig. 6, the HDS reaction of DBT can be categorized into two primary pathways [35,36]. The first pathway is the hydrogenation pathway, in which DBT undergoes a series of reactions involving partial hydrogenation and subsequent breakage of the C—S bond. The completely saturated BCH is created as a result of further hydrogenation that follows this step. The DBT second method, known as the direct desulfurization (DDS) pathway, avoids hydrogenating the benzene ring. Another route is the DDS pathway of DBT, which yields BP by breaking the C—S bond directly without hydrogenating the benzene ring.

An analysis was conducted of the reaction of DBT over Pt/Al_2O_3 catalyst at varying reaction temperatures and pressures after 60 min, the results of which are presented in Fig. 7. It was

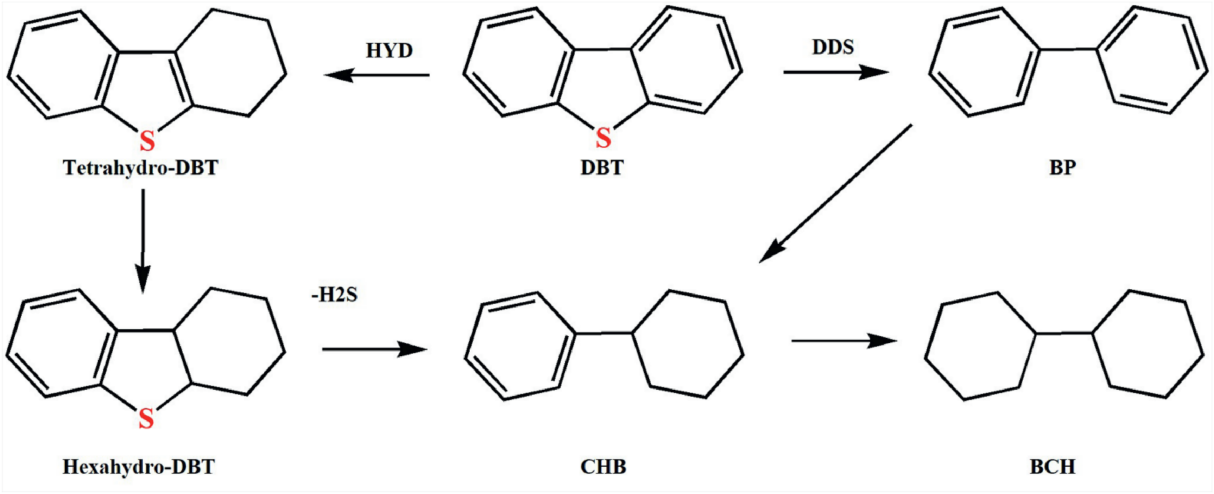

Fig. 6. DBT HDS reaction pathway.

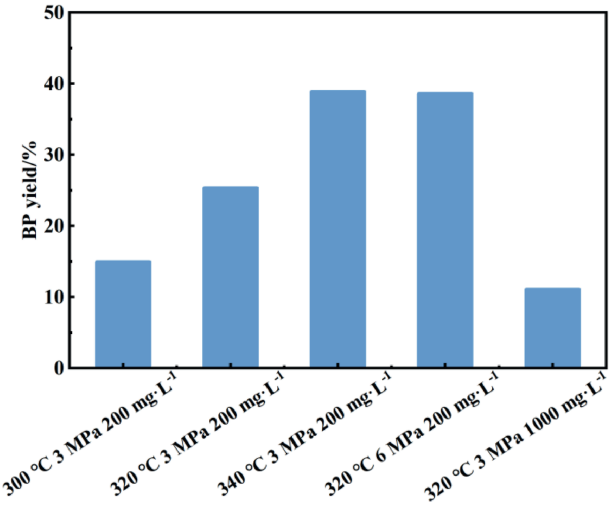

Fig. 7. The BP yields of the products after 60 min at varying temperatures and pressures.

determined that as the temperature rose, the BP yield of the direct desulfurization product gradually increased, reaching 14.93% and 25.36% at 300 °C and 320 °C, respectively. When heated to 340 °C, the BP yield attained 38.89%. A trace quantity of BCH is present in the reaction product; however, BCH can also be obtained from the hydrogenation saturation of BP, in addition to the HDS pathway. The absence of the product CHB in the reaction indicates that BCH was likely generated by the hydrogenation of BP at an elevated reaction pressure. The results obtained thus far demonstrate that the DBT HDS reaction proceeds *via* DDS pathway over the catalyst. Furthermore, an increase in reaction pressure has been shown to enhance the BP yield. However, when the S content was increased to 1000 mg·L^{-1}, the reaction activity decreased rapidly, and the yield of the desulfurization product BP was only 11.11%.

3.4. Mechanism of DBT inhibition on hydrodenitrogenation reaction

According to a subsequent examination of the reaction rate constants after DBT was added, the rate of 14THQ hydrogenation reaction was accelerated, while the rate of Q hydrogenation reaction showed a slight decrease. The initial step rate constants k_2 and k_5 for 14THQ hydrogenation bond breaking and direct bond breaking both decreased by one order of magnitude, indicating that the adsorption activation of the reactant 14THQ was greatly impacted by the addition of DBT. The analyses suggest that there should be a competition between 14THQ and DBT for adsorption on the catalyst surface. A preceding study established that 4,6-dimethyltetrahydrodibenzothiophene exhibited an inhibition of 2-methylpyridine hydrogenation, leading to the formation of 2-methylpiperidine. However, this compound did not demonstrate any influence on the C—N bond breakage during 2-methylpiperidine HDN [37]. The researchers [38,39] posited that following the HDS reaction on a Pt metal surface, an unstable Pt-S bond is formed. When there are high levels of hydrogen present on the surface, the sulfur atoms migrate to form hydrogen sulfide with the active hydrogen, thereby ensuring the platinum remains in the metal state without being poisoned by sulfur. It is evident that DBT will occupy a significant proportion of active sites during the adsorption activation at the surface [22,40], thereby reducing the number of nitrogen-containing compounds adsorption activation sites. This, in turn, will result in a decline in reaction activity.

A detailed analysis of the rate constant k_7 for the bond-breaking primitive step reveals that its value is considerably higher than that of the reaction without the addition of DBT, indicating that the addition of DBT is a promoter for the bond-breaking step [41–43]. The underlying reason for this observation is that the DBT HDS reaction will form H_2S within the reaction system, which might be broken down to produce H^+ on the catalyst surface. In our previous study [26], we established that the presence of H^+ is an essential step for the breaking of C—N bonds, hence the presence of H_2S promotes the breaking of C—N bonds. This conclusion is in line with the findings of some researchers on sulfide catalysts.

The adsorption on the catalyst surface was further confirmed by theoretical calculations to confirm the previously reported conclusion about the presence of competitive adsorption. The outcomes are shown in Fig. 5. The findings revealed that DBT exhibited optimal stability in the hcp adsorption configuration on the Pt surface, accompanied by an adsorption energy of −1.78 eV. In the previously mentioned technique, it was discovered that the adsorption energies of DBT and 14THQ were nearly identical, thereby substantiating the hypothesis that both compounds would engage in competition for adsorption on the catalyst surface, ultimately resulting in a reduction in the reaction rate.

3.5. Catalysts for mitigating inhibition

The present study investigates the inhibition of a HDN process catalyzed by Pt/Al_2O_3 catalyst, resulting from the adsorption of NP or DBT on the catalyst surface. Kinetic study emphasizes the significance of active sites on the catalyst surface and the adsorption of molecules containing nitrogen, which shows that this competitive adsorption lowers HDN activity. The 10cTi-PtAl catalyst was prepared by TiO_2 deposition on the Pt/Al_2O_3 surface using ALD, which exhibited superior nitrogen-containing compound adsorption and elevated C—N bond breaking capacity with enhanced reaction stability. In previous studies, the adsorption capacity of the material for nitrogen-containing compounds has been the focus of analysis. [26]. Consequently, the HDN activity following the addition of aromatics or sulfur-containing substances was examined on this catalyst, with the intention of reducing inhibition and increasing the reaction total activity. The reactions on the modified catalysts were carried out at 320 °C and 3 MPa.

3.5.1. Effect of naphthalene on the hydrodenitrogenation reaction

The HDN reaction of 14THQ following the addition of aromatics/sulfur-containing compounds was carried out over a 10cTi-PtAl catalyst, and the yields of the products DHQ and PCH after 4 h of reaction are shown in Fig. 8. Firstly, the yields of DHQ and PCH on this catalyst were compared before and after the addition of NP. The results demonstrated that the yield of DHQ underwent a change from a gradual decrease to a gradual increase following the addition of NP. This indicated that the reaction rate of HDN was reduced, which led to a decrease in the yield of the intermediate product DHQ and the reaction was in the preliminary hydrogenation stage. Furthermore, the phenomenon of the rapid breaking of the bond of DHQ that caused a decrease in its concentration did not occur. The yield of PCH exhibited a gradual increase over time. However, the addition of NP resulted in a decline in the overall PCH yield, accompanied by a decrease to 50.94% of the initial bond-breaking activity. A comparison of the activity changes after the addition of NP to the Pt/Al_2O_3 catalyst revealed that the bond-breaking activity decreased to 27.10% of the original value, while the TiO_2-modified catalyst mitigated the inhibitory effect of NP on the HDN reaction, resulting in a significant improvement in nitrogen removal activity.

The yields of NP hydrogenation products on the catalyst were examined in order to determine the impact of the TiO_2-modified catalyst on NP during the HDN process. The findings are shown in Table 3. The table data shows that the yields of tetralin and decalin hydrogenation products can reach 59.22% after 4 h of reaction, with the yield of decalin reaching 2.52%. Under the same reaction conditions, the yields of tetralin and decalin on the Pt/Al_2O_3 catalyst were 57.27% and 0.84%, respectively. Therefore, the deposition of TiO_2 not only improves the performance of the HDN reaction, but also enhances the performance of naphthalene hydrogenation. The previous study [26] demonstrated that catalysts deposited with TiO_2 exhibited superior hydrogen overflow performance, resulting in enhanced hydrogenation performance. This boosted the hydrogenation process of 14THQ in addition to improving the hydrogenation of NP, increased the concentration of DHQ products, and further improved the activity of the bond-breaking reaction. Furthermore, the deposition of TiO_2 introduced a novel bond-breaking active site, the Ti^{3+}-$Pt^{\delta-}$site, which caused the increased bond-breaking activity. In conclusion, the TiO_2-modified catalyst is able to mitigate the impact of NP on the HDN reaction and enhance the bond-breaking activity of HDN, as well as the activity of the NP hydrogenation reaction.

Table 3
Yields of NP hydrogenation products over 10cTi-PtAl catalysts.

Reaction time/h	Tetralin yield/%	Decalin yield/%
1	14.08	0.46
2	23.86	0.46
3	42.84	1.37
4	59.22	2.52

3.5.2. Effect of dibenzothiophene on the hydrodenitrogenation reaction

The HDN reaction with DBT was carried out over 10cTi-PtAl catalyst, and the results are presented in Fig. 8. It is evident that both the DHQ and PCH yields gradually increased over time. In the absence of DBT, the PCH yield decreased to 14.11%, while the bond-breaking activity in Pt/Al_2O_3 decreased to 10.5%. Following the application of TiO_2, the catalyst's bond-breaking activity increased, indicating that the addition of Ti species somewhat mitigated DBT's inhibiting impact on the HDN process. The decline in DHQ yield indicates the presence of ongoing competition between DBT and 14THQ for adsorption at the surface.

The HDS product yield of DBT was examined in order to look into the mechanism following TiO_2 deposition. The yield of BP product was found to be 26.47%, 33.81%, 43.90% and 51.50% from 1

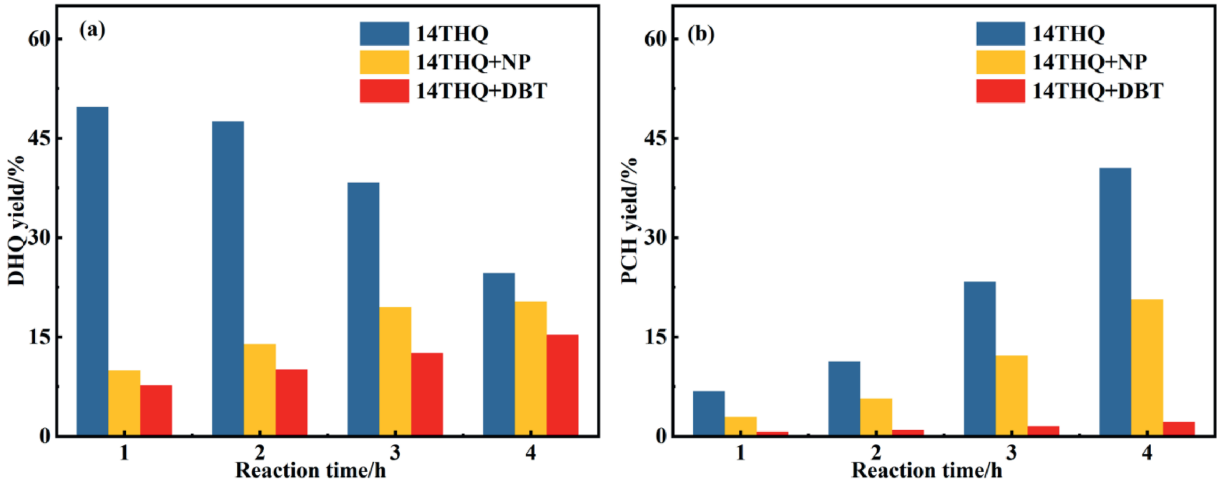

Fig. 8. Yield of DHQ and PCH on 10cTi-PtAl catalyst after addition of NP or DBT.

to 4 h, respectively. It can be observed that the desulfurization reaction occurs in the direct bond breaking path, and as the reaction proceeded gradually, the yield of the product BP was achieved. Under the same reaction conditions, the yield on the Pt/Al_2O_3 catalyst was 50.81%, indicating a small increase in the direct bond-breaking activity after deposition of TiO_2. A comparison of the enhancement of activity on the catalyst during NP hydrogenation reveals that the catalyst after deposition of TiO_2 exhibits a significant enhancement of hydrogenation performance due to higher hydrogen overflow. The enhancement of the C–N breaking activity creates a bond-breaking active site for the deposition of TiO_2. However, it is not possible to determine whether this active site is in charge of increasing the C–S bond breaking activity.

4. Conclusions

This study elucidates the distinct inhibition mechanisms of aromatic and sulfur-containing compounds on 14THQ HDN over Pt-based catalysts. Experimental investigations revealed that the addition of NP, selected as the aromatic model compound, exerts significant inhibitory effects on HDN efficiency. Systematic evaluation demonstrated that thermal activation effectively alleviates this inhibition, whereas pressure modulation exerts negligible influence—confirming surface adsorption competition as the rate-limiting factor. Kinetic analyses established that the hydrogenation of 14THQ to DHQ exhibited a tenfold reduction in reaction rate constant, identifying this step as the critical inhibition pathway. DFT calculations corroborated that HDN activity reduction originates from competitive adsorption between 14THQ and NP at catalytic active sites. A marginal decrease in the intrinsic C–N bond cleavage rate was attributed to steric hindrance induced by DHQ adsorption, which occupies surface sites and diminishes bond-breaking activity. Sulfur-containing compounds have been found to inhibit the HDN reaction to a greater extent than aromatic hydrocarbons. However, it has been observed that this inhibition decreases with increasing temperature and is unaffected by pressure changes. Kinetic studies demonstrated that DBT inhibited 14THQ hydrogenation and direct bond breaking. In this process, 14THQ hydrogenation reduced the reaction rate constant for DHQ by an order of magnitude, thus constituting a pivotal step in the inhibition. This suggests that DBT occupies numerous active sites during surface adsorption and activation, thereby reducing the amount of adsorbed and activated nitrogen-containing compounds. It is noteworthy that the addition of DBT facilitates the primitive step of C–N bond breaking. The fundamental process is the cleavage of H_2S, which is started by the elimination of substances that contain sulfur and produces H^+. Atomic-layer-deposited TiO_2-modified Pt/Al_2O_3 catalysts effectively mitigate NP/DBT-induced inhibition through three synergistic effects: (1) enhanced nitrogen-selective adsorption capacity, (2) optimized hydrogen spillover, and (3) creation of supplementary C–N bond cleavage sites. This multifunctional design strategy successfully addresses competitive adsorption limitations, providing critical insights for sulfur/aromatic-resistant HDN catalyst development.

CRediT Authorship Contribution Statement

Yifan Xue: Writing – original draft, Methodology, Formal analysis, Conceptualization. Fei Zhao: Validation, Data curation. Jie Feng: Supervision, Resources, Investigation, Conceptualization. Wenying Li: Writing – review & editing, Project administration, Funding acquisition.

Declaration of Competing Interest

The authors declare that they have no known competing financial interests or personal relationships that could have appeared to influence the work reported in this paper.

Acknowledgements

This work was supported by the Key Project of National Natural Science Foundation of China (22038008), the Science and Technology Innovation Project of National Energy Group China Shenhua Coal to Oil Chemical Co. (MZYHG-2021-01), and the Program of Beijing Huairou Laboratory (ZD2023012A).

Nomenclature

E_{ads}	adsorption energy
P	pressure
T	temperature
t	reaction time

Supplementary Material

Supplementary data to this article can be found online at https://doi.org/10.1016/j.cjche.2025.09.037.

References

[1] K.C. Xie, W.Y. Li, W. Zhao, Coal chemical industry and its sustainable development in China, *Energy* 35 (11) (2010) 4349–4355.
[2] K. Guo, Y. Ding, Z.X. Yu, One-step synthesis of ultrafine MoNiS and MoCoS monolayers as high-performance catalysts for hydrodesulfurization and hydrodenitrogenation, *Appl. Catal., B* 239 (2018) 433–440.
[3] T.A. Zepeda, B. Pawelec, R. Obeso-Estrella, J.N.D.d. León, S. Fuentes, G. Alonso-Núñez, J.L.G. Fierro, Competitive HDS and HDN reactions over NiMoS/HMS-Al catalysts: diminishing of the inhibition of HDS reaction by support modification with P, *Appl. Catal., B* 180 (2016) 569–579.
[4] V.A. Vallés, B.C. Ledesma, G.A. Pecchi, O.A. Anunziata, A.R. Beltramone, Hydrogenation of tetralin in presence of nitrogen using a noble-bimetallic couple over a Ti-modified SBA-15, *Catal. Today* 282 (2017) 111–122.
[5] W. Wang, H.F. Li, W. Han, L. Zhang, M.F. Li, A DFT study of the adsorption behavior of sulfur and nitrogen compounds on the NiMoS phase, *China Pet. Process. Petrochem. Technol.* 22 (1) (2020) 40–48.
[6] G. de Souza Guedes Junior, I. Gigante Nascimento, M. Ahmad, C. Killeen, J.A. Boscoboinik, J. Trelewicz, J.C. Pinto, M. Dorneles de Mello, M. Antunes Pereira da Silva, Kinetics of simultaneous hydrodesulfurization and hydrodenitrogenation reactions using CoMoP/Al_2O_3 and NiMoP/Al_2O_3, *Chem. Eng. Sci.* 275 (2023) 118725.
[7] E.M. Morales-Valencia, O.J. Vargas-Montañez, P.A. Monroy-García, L.G. Avendaño-Barón, E.A. Quintero-Quintero, C. Elder-Bueno, A.Y. Santiago-Guerrero, V.G. Baldovino-Medrano, Conditions for increasing the hydrodesulfurization of dibenzothiophene when co-feeding naphthalene, quinoline, and indole, *J. Catal.* 404 (2021) 204–209.
[8] C.N. Satterfield, M. Modell, J.F. Mayer, Interaction between catalytic hydrodesulfurization of thiophene and hydrodenitrogenation of pyridine, *AIChE J.* 21 (6) (1975) 1101–1107.
[9] S. Shin, H. Yang, K. Sakanishi, I. Mochida, D.A. Grudoski, J.H. Shinn, Inhibition and deactivation in staged hydrodenitrogenation and hydrodesulfurization of medium cycle oil over NiMoS/Al_2O_3, *Appl. Catal., A* 205 (1) (2001) 101–108.
[10] V.L. Vopa, C.N. Satterfield, Poisoning of thiophene hydrodesulfurization by nitrogen compounds, *J. Catal.* 110 (2) (1988) 375–387.
[11] E. Furimsky, F.E. Massoth, Deactivation of hydroprocessing catalysts, *Catal. Today* 52 (4) (1999) 381–495.
[12] C. Kwak, J.J. Lee, J.S. Bae, S.H. Moon, Poisoning effect of nitrogen compounds on the performance of CoMoS/$A1_2O_3$ catalyst in the hydrodesulfurization of dibenzothiophene, 4-methyldibenzothiophene, and 4,6-dimethyldibenzothiophene, *Appl. Catal., B* 35 (1) (2001) 59–68.
[13] P. Zeuthen, K.G. Knudsen, D.D. Whitehurst, Organic nitrogen compounds in gas oil blends, their hydrotreated products and the importance to hydrotreatment, *Catal. Today* 65 (2-4) (2001) 307–314.
[14] C.L.S. Georgina, D.l.R.H. Antonio, C.D. Luis, J.C.M. J, Inhibition effects of nitrogen compounds on the hydrodesulfurization of dibenzothiophene, *Appl. Catal., A* 207 (1-2) (2001) 103–112.
[15] G.C. Laredo, E. Ahamirano, D.l.R.J. Antonio, Inhibition effects of nitrogen compounds on the hydrodesulfurization of dibenzothiophene: part 2, *Appl. Catal., A* 243 (2) (2003) 207–214.

[16] M. Nagai, T. Sato, A. Aiba, Poisoning effect of nitrogen compounds on dibenzothiophene hydrodesulfurization on sulfided $NiMo/Al_2O_3$ catalysts and relation to gas-phase basicity, *J. Catal.* 97 (1986) 52–58.
[17] T. Kabe, K. Akamatsu, A. Ishihara, S. Otsuki, M. Godo, Q. Zheng, W.H. Qian, W.H. Qian, Deep hydrodesulfurization of light gas oil. 1. Kinetics and mechanisms of dibenzothiophene hydrodesulfurization, *Ind. Eng. Chem. Res.* 36 (12) (1997) 5146–5152.
[18] M. Nagai, High activity and selectivity of a "poisoned" $NiMo/Al_2O_3$ catalyst for a desulfurization reaction, *Ind. Eng. Chem. Prod. Res. Dev.* 24 (3) (1985) 489–491.
[19] N. Salazar, S.B. Schmidt, J.V. Lauritsen, Adsorption of nitrogenous inhibitor molecules on MoS2 and CoMoS hydrodesulfurization catalysts particles investigated by scanning tunneling microscopy, *J. Catal.* 370 (2019) 232–240.
[20] S. Rangarajan, M. Mavrikakis, DFT insights into the competitive adsorption of sulfur- and nitrogen-containing compounds and hydrocarbons on co-promoted molybdenum sulfide catalysts, *ACS Catal.* 6 (5) (2016) 2904–2917.
[21] A. Infantes-Molina, A. Romero-Pérez, E. Finocchio, G. Busca, A. Jiménez-López, E. Rodríguez-Castellón, HDS and HDN on SBA-supported RuS_2 catalysts promoted by Pt and Ir, *J. Catal.* 305 (2013) 101–117.
[22] J. Liu, W.Y. Li, J. Feng, X. Gao, Z.Y. Luo, Promotional effect of TiO_2 on quinoline hydrodenitrogenation activity over $Pt/\gamma\text{-}Al_2O_3$ catalysts, *Chem. Eng. Sci.* 207 (2019) 1085–1095.
[23] X.D. Liu, X.Y. Fan, L. Wang, J.X. Sun, Q. Wei, Y.S. Zhou, W.B. Huang, Competitive adsorption between sulfur- and nitrogen-containing compounds over NiMoS nanocluster: the correlations of electronegativity, morphology and molecular orbital with adsorption strength, *Chem. Eng. Sci.* 231 (2021).
[24] Q. Yao, C.L. Wang, H.W. Wang, H. Yan, J. Lu, Revisiting the Au particle size effect on TiO_2-coated Au/TiO_2 catalysts in CO oxidation reaction, *J. Phys. Chem. C* 120 (17) (2016) 9174–9183.
[25] C.L. Wang, H.W. Wang, Q. Yao, H. Yan, J. Li, J. Lu, Precisely applying TiO_2 overcoat on supported Au catalysts using atomic layer deposition for understanding the reaction mechanism and improved activity in CO oxidation, *J. Phys. Chem. C* 120 (1) (2016) 478–486.
[26] Y.F. Xue, J. Feng, J.Y. Ma, W.Y. Li, Elucidation of C–N bond cleavage mechanism in quinoline hydrodenitrogenation over Pt-based catalysts, *Chem. Eng. Sci.* 285 (2024).
[27] Y.F. Xue, J. Feng, Y.C. Song, W.Y. Li, Effect of noble metal nanoparticle size on C–N bond cleavage performance in hydrodenitrogenation: a study of active sites, *Front. Chem. Sci. Eng.* 17 (12) (2023) 1986–2000.
[28] J. Liu, W.Y. Li, J. Feng, X. Gao, Molecular insights into the hydrodenitrogenation mechanism of pyridine over $Pt/\gamma\text{-}Al_2O_3$ catalysts, *Mol. Catal.* 495 (2020) 111148.
[29] D. Xie, X. Liu, H. Lv, Y. Guo, Products, pathways, and kinetics for catalytic hydrodenitrogenation of quinoline in hydrothermal condition, *J. Supercrit. Fluids* 182 (2022).
[30] J.G. Dickinson, J.T. Poberezny, P.E. Savage, Deoxygenation of benzofuran in supercritical water over a platinum catalyst, *Appl. Catal., B* 123-124 (2012) 357–366.
[31] H.X. Yin, C.H. Zhang, H.B. Yin, D.Z. Gao, L. Shen, A.L. Wang, Hydrothermal conversion of glycerol to lactic acid catalyzed by Cu/hydroxyapatite, Cu/MgO, and Cu/ZrO_2 and reaction kinetics, *Chem. Eng. J.* 288 (2016).
[32] B.C. Ledesma, O.A. Anunziata, A.R. Beltramone, HDN of indole over Ir-modified Ti-SBA-15, *Appl. Catal., B* 192 (5) (2016) 220–233.
[33] M.J. Guttieri, W.F. Maier, Selective cleavage of carbon-nitrogen bonds with platinum, *J. Org. Chem.* 49 (16) (1984) 2875–2880.
[34] M.S. Rana, R. Navarro, J. Leglise, Competitive effects of nitrogen and sulfur content on activity of hydrotreating $CoMo/A_{l2}O_3$ catalysts: a batch reactor study, *Catal. Today* 98 (1-2) (2004) 67–74.
[35] O.Y. Gutiérrez, S. Singh, E. Schachtl, J. Kim, E. Kondratieva, J. Hein, J.A. Lercher*, Effects of the support on the performance and promotion of $(Ni)MoS_2$ catalysts for simultaneous hydrodenitrogenation and hydrodesulfurization, *ACS Catal.* 4 (5) (2014) 1487–1499.
[36] W. Han, H. Nie, X.Y. Long, M.F. Li, Q. Yang, D.D. Li, Effects of the support Brønsted acidity on the hydrodesulfurization and hydrodenitrogention activity of sulfided $NiMo/Al_2O_3$ catalysts, *Catal. Today* 292 (2017) 58–66.
[37] M. Egorova, R. Prins, Competitive hydrodesulfurization of 4,6-dimethyldibenzothiophene, hydrodenitrogenation of 2-methylpyridine, and hydrogenation of naphthalene over sulfided $NiMo/\gamma\text{-}Al_2O_3$, *J. Catal.* 224 (2) (2004) 278–287.
[38] V.G. Baldovino-Medrano, S.A. Giraldo, A. Centeno, The functionalities of $Pt/\gamma\text{-}Al_2O_3$ catalysts in simultaneous HDS and HDA reactions, *Fuel* 87 (10-11) (2008) 1917–1926.
[39] T. Kabe, W.H. Qian, Y. Hirai, L. Li, A. Ishihara, Hydrodesulfurization and hydrogenation reactions on noble metal catalysts: I. Elucidation of the behavior of sulfur on alumina-supported platinum and palladium using the ^{35}S radioisotope tracer method, *J. Catal.* 190 (1) (2000) 191–198.
[40] S. Humbert, G. Izzet, P. Raybaud, Competitive adsorption of nitrogen and sulphur compounds on a multisite model of NiMoS catalyst: a theoretical study, *J. Catal.* 333 (2016) 78–93.
[41] A. Hrabar, J. Hein, O.Y. Gutiérrez, J.A. Lercher, Selective poisoning of the direct denitrogenation route in *o*-propylaniline HDN by DBT on Mo and $NiMo/\gamma\text{-}Al_2O_3$ sulfide catalysts, *J. Catal.* 281 (2) (2011) 325–338.
[42] M. Egorova, R. Prins, Mutual influence of the HDS of dibenzothiophene and HDN of 2-methylpyridine, *J. Catal.* 221 (1) (2004) 11–19.
[43] P.F. Zhang, Y.S. Zhou, R.X. Zhang, X.Y. Fan, Q. Wei, X.D. Liu, Effect of sulfur compounds on the hydrodenitrogenation of 1,2,3,4-tetrahydroquinoline and its intermediates over $NiMo/Al_2O_3$ catalyst, *Fuel* 277 (2020) 118186.